

*This paper was recommended for publication in revised form by Regional Editor Lian-Ping Wang*

## **CENTRIFUGAL DEPOSITION OF IRON OXIDE MAGNETIC NANORODS FOR HYPERTHERMIA APPLICATION**

**Eric Duong**

Department of Mechanical Engineering,  
California State Polytechnic University, Pomona  
3801 W Temple Avenue, Pomona, CA 91768, USA

**Sophia Y. Chan**

Department of Mechanical Engineering,  
California State Polytechnic University, Pomona  
3801 W Temple Avenue, Pomona, CA 91768, USA

**\* Yong X. Gan**

Department of Mechanical Engineering,  
California State Polytechnic University, Pomona  
3801 W Temple Avenue, Pomona, CA 91768, USA

**Lihua Zhang**

Center for Functional Nanomaterials,  
Brookhaven National Laboratory,  
Upton, NY 11973, USA

*Keywords: Centrifugal deposition; iron oxide; magnetic nanorods; external field induced heating; hyperthermia*

*\* Corresponding author: Department of Mechanical Engineering, California State Polytechnic University, Pomona  
3801 W Temple Avenue, Pomona, CA 91768, USA, Phone: +1-909-869-2388, Fax: +1-909-869-4341,  
E-mail address: yxgan@csupomona.edu*

### **ABSTRACT**

Centrifugal deposition of iron oxide was performed to manufacture magnetic nanorods in an aqueous solution. The nanorods were examined by electron microscopy. The diameter of the nanorods ranges from 10 to 20 nm. The length is about 150 nm. The nanorods were incorporated into a silicone polymer to simulate body tissues injected with magnetic nanomaterials. Then the magnetic nanorod-containing silicone samples were put into a microwave to examine the external electromagnetic field induced heating behavior. Dramatic increase in temperature was observed when the nanorods were exposed to the external electromagnetic field for 2 seconds. It is concluded that the nanorods generate intensive heating effect and they have the potential for hyperthermia application.

### **INTRODUCTION**

Centrifugal deposition as a relatively new technology for manufacturing nanomaterials has caught much attention due to its simplicity in equipment and process control. The feasibility of using centrifugal or rotational effect to make micro- and nanoscale fibers was demonstrated [1]. Desirable monolayer and multilayer gold nanoparticle films can also be obtained by using the simple centrifugal deposition method [2]. Typically, centrifugal force causes newly formed materials to aggregate

along certain preferential directions at the surface of any existing supporting substrate. This allows the self-assembled structure formation as shown in the work performed by Chang et al. [3]. Centrifugal forces may generate complex effects on the formation of nanostructures. For example, a centrifugal force of less than one gravitational force was generated by a rotary reactor for atomic layer depositing  $\text{Al}_2\text{O}_3$  on large quantities of  $\text{ZrO}_2$  nanoparticles [4]. At such a low level, the centrifugal force caused the particles being agitated by a continuous “avalanche” of particles, which promotes the deposition of  $\text{Al}_2\text{O}_3$  layer on  $\text{ZrO}_2$  nanoparticles. Although significant efforts have been made on nanomaterial processing by various manufacturing techniques, much less work has been reported about the structure evolution during centrifugal deposition. Since the direct formation of magnetic nanorods under the action of centrifugal forces has the advantage of being easy to control, a low cost manufacturing process for large scale production of nanomaterials can be expected.

Electromagnetic hyperthermia has been attracting significant attention in treating cancerous cells due to its non-invasive and quick recovery time. Reducing and eliminating cancer cells have been studied extensively by radiation treatment and/or chemical treatment. These treatments are called radiation therapy [1] and chemotherapy [2]. They harm

the non-effective area as a result of the high dosage or poisonous drugs used during the treatment processes. Consequently, they damage the normal cells of patients and recovery takes long time. A possible solution is magnetic hyperthermia [3,4]. It is a non-invasive process that is targeted to a specific area for treatment. Only the cancerous cell is being treated and leaving the non-infected parts exposed from damages. Besides using the iron oxide superparamagnetic nanoparticle [5], a combination of several particles or ferrite compounds is delivered into the target cell [6-9]. In addition, hydroxyapatite (HAP) has recently been investigated as a drug carrier for combined chemo- and hyperthermia therapy [10]. The elements are highly responsive to electromagnetic field which causes the element to heat up in short amount of time. The heat then damages or destroys malignant tissues without causing harm to the surrounding cells. Hyperthermia increases oxygen by dilating blood cells and the warmth increase blood flow. Therefore, it helps delivery response to medication.

In this work, our focus is on centrifugal deposition of iron oxide based magnetic nanomaterial with the potential hyperthermia functionality [15]. Hyperthermia has found two types of application in cancer treatments. One is the use of heat to kill cancer cells directly [16-21]. The other is to use the magnetic nanoparticle-based hyperthermia to generate local heat resulting in the release of drugs [22]. The mechanisms of hyperthermia of magnetic nanomaterials were proposed [23], but they are specifically applicable for nanoparticles. Until now, much less work was reported on understanding the behavior of nanorods embedded in tissues. We used simulated tissues to characterize the hyperthermia behavior of the centrifugal deposited nanomaterial. The nanomaterial was injected into a silicone polymer. After the polymer was cured in ambient condition for 24 h, an induction heating experiment was performed to investigate how fast the temperature changes due to the existence of the external electromagnetic field.

## MATERIALS AND EXPERIMENTAL METHODS

Iron (III) nitrate nonahydrate with the chemical formula of  $\text{Fe}(\text{NO}_3)_3 \cdot 9\text{H}_2\text{O}$ , and potassium hydroxide, KOH, ACS agent were ordered from Alfa Aesar-A Johnson Matthey Company. In the 1st step of the process, 3 grams of KOH + 5 mL of deionized water were mixed in test tube No.1. This step was then repeated but now required 9 grams of  $\text{Fe}(\text{NO}_3)_3 \cdot 9\text{H}_2\text{O}$  + 15 mL of deionized water to be mixed in test tube No.2. Nanoparticle seeds were formed by transferring the KOH solution from test tube No. 1 to the other (test tube No. 2). The initiation of the iron hydroxide nanoparticle seeds started at the  $\text{Fe}(\text{NO}_3)_3 \cdot 9\text{H}_2\text{O}/\text{KOH}$  interface. Then, the test tube contains iron hydroxide nanoparticle seeds was introduced to a centrifuge machine running at 3300 rpm for 15 minutes. Through the centrifuge process the nanoparticles moved from the interface toward the bottom of the glass tube. Nanorods were generated from the growth of the nanoparticles during the centrifugal motion. The nanorods were separated from the solution under the action of the centrifugal force. After pouring

the solution out, the nanorods remain at the bottom of the tube. Then, 7.5 mL of deionized water was added to the test tube and placed into the centrifuge for another 15 minutes at 3300 rpm. The purpose of using deionized water was to remove the residues of potassium nitrate left by the reaction. This purification process was repeated for three times. The test tube was then taken out of the centrifuge and set on a hotplate. This allowed the iron hydroxide nanorods to dry and change into iron oxide nanorods.

With the fabrication of the nanorods completed, the next step was to simulate the process of magnetic nanostructure-based hyperthermia through the following test procedures. To perform the test, 3 sets of samples in the cylindrical disk with a dimension of  $\Phi 25 \times 5$  (mm) were made by mixing a silicone polymer with different weight percentages of nanorods. The silicone polymer was used because it exhibits good compatibility with human tissues. Additional samples containing only the silicon polymer was also prepared as the control specimens for obtaining the baseline of temperature tests. With the use of a standard 900 W microwave, each sample was individually introduced to electromagnetic waves to examine the heat generation behavior.

## RESULTS AND DISCUSSION

In Figure 1, it schematically shows how the nanorods form during the centrifugal process. Also shown is a photograph of the prepared nanomaterial. Obviously, the drag generated by the centrifugal action allows the product to become elongated clusters, which facilitates the formation of the nanorods.

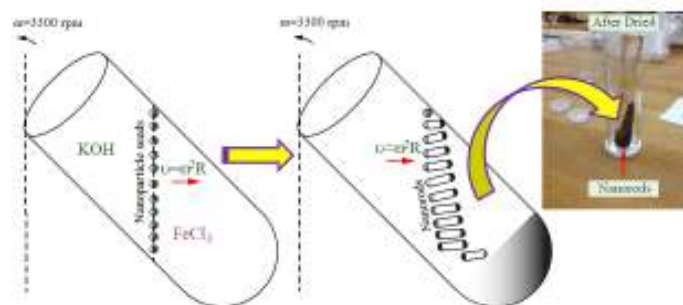
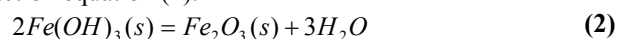


Figure 1 Schematic and photograph showing the centrifugal process and the prepared nanomaterial.

With the reaction of iron (III) nitrate nonahydrate and potassium hydroxide, a solution of iron hydroxide, potassium nitrate and water is produced as shown in the following reaction equation:



Being air-dried on the hot plate, the iron hydroxide converts into iron oxide through the reaction as shown in reaction equation (2).



In order to verify the formation of nanorods under the action of the centrifugal force, the final product was examined using transmission electron microscopy (TEM). The TEM analysis results are shown in Figure 2. In Figure 2(a), the electron microscopic image shows the surface morphology of the iron oxide nanorods. The average length of the nanorods is about 100 nm. The radii of the nanorods are in the range from 10 nm to 20 nm. The average aspect ratio (length to diameter) of the nanorods is about 10. In Figure 2(b), the formation of clusters of iron oxide nanorods was illustrated. This indicates the transition from nanorods to bundles of nanorods or nanoflakes.

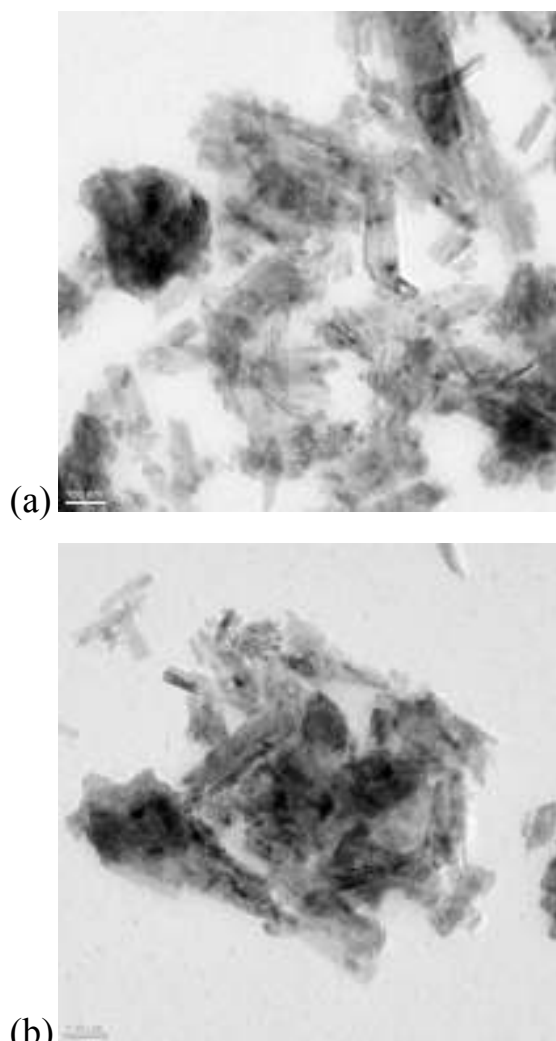


Figure 2 TEM images of the centrifugal deposited iron oxide nanorods: (a) in dispersed form, (b) in bundles.

Qualitative analysis of the elements using energy dispersive X-ray diffraction technique was performed to confirm the chemical composition of the nanostructure. The results are presented in Figure 3. It is evident that the energy dispersive X-ray diffraction spectrum of the iron oxide nanorods shows the major elements of Fe and O. The Cu signal comes from the

TEM sample holder. K peak is also observed, which comes from the residue of  $\text{KNO}_3$  in the nanorods.

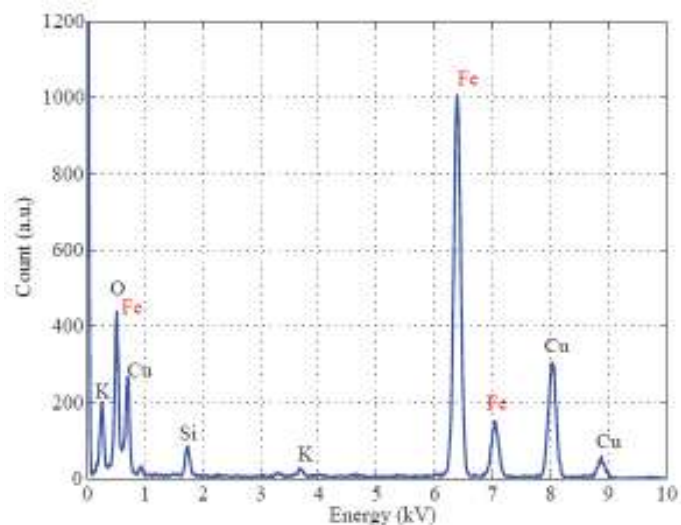


Figure 3 Energy dispersive X-ray diffraction spectrum of the nanorod.

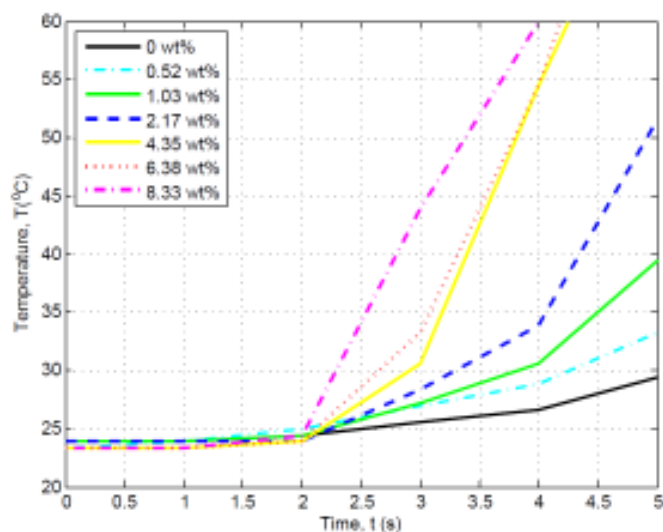


Figure 4 External electromagnetic field induced temperature change.

Figure 4 shows the temperature test results for various kinds of specimens. Working on different concentrations of the magnetic nanorods, one assumes the sample with the highest concentration of magnetic nanorods be the first to reach high temperatures versus the low concentration samples. Heat dissipation from magnetic nanorods is known as the cause by the delay in the relaxation time of the magnetic moment through the rotation within the nanorods or the rotation of the nanorods themselves when they are excited by a magnetic field. The results as shown in Figure 4 confirm the concentration effect. The higher the concentration of iron oxide, the faster the temperature increases.

The heat that is dissipated is closely related to the relaxation time which relies on nanorod diameter. The specimens that were made in this work have the stoichiometric composition of  $\text{Fe}_2\text{O}_3$ . The comparison of temperature increase due to the excitation by external field is shown in Figure 4. As can be seen, the time needed for magnetic excitation is about 2 s. Specimens without the addition of magnetic nanorods did not show the same extent of increase in temperature. To estimate how much heat is generated, analysis of the heat dissipation of a single magnetic nanorod using fundamental equations of heat transfer to calculate the heat rate was performed and the results are presented in Figure 5. Compared with other research results, the sample in our work generates heat much faster. For example, typical response time for magnetic field induced heating is about 6 minutes [16]. But in this work, the response time is reduced to seconds. This indicates that even the lowest concentration of 0.25 wt% of the magnetic nanorods is enough for generating significant heating effect.

## CONCLUSIONS

Iron oxide nanorods have been successfully manufactured by centrifugal deposition from aqueous solution. The aspect ratio of the nanorods is about 10. The nanorods are responsive to external electromagnetic field. When they are embedded into silicone polymer as the simulated tissue material, effective hyperthermia behavior was confirmed. The higher the concentration of the nanorods, the faster the temperature increases. For all the three types of samples with the concentrations of 4.348%, 6.383% and 8.333%, the hyperthermia behavior can be observed within 2 s. The sample with the highest concentration of nanorods shows the highest heat generation rate of 1.93 W/mm<sup>2</sup>.

## ACKNOWLEDGMENTS

This work is supported by the U.S. National Science Foundation (NSF) under Grant No. CMMI-1333044. The electron microscopic research carried out at the Center for Functional Nanomaterials, Brookhaven National Laboratory is supported by the U.S. Department of Energy, Office of Basic Energy Sciences under Contract No. DEAC02-98CH10886. YXG also acknowledges the support by the CAFA Faculty Development Grant and the California State Polytechnic University, Pomona 2013-2014 President's Research, Scholarship and Creative Activity Program Grant.

## REFERENCES

[1] T.B. Míndru, L. Ignat, I.B. Míndru, M. Pinteala, Morphological aspects of polymer fiber mats obtained by air flow rotary-jet spinning, *Fiber Polym.* 14 (2013) 1526-1534.  
 [2] I.C. Ni, S.C. Yang, C.W. Jiang, C.S. Luo, W. Kuo, K.J. Lin, S.D. Tzeng, Formation mechanism, patterning, and physical properties of gold-nanoparticle films assembled by an interaction-controlled centrifugal method, *J. Phys. Chem. C* 116 (2012) 8095–8101.

[3] J.H. Chang, C.R. Aleman de Leon, I.W. Hunter, Self-assembled, nanostructured polypyrrole films grown in a high-gravity environment, *Langmuir* 28 (2012) 4805-4810.

[4] J.A. McCormick, B.L. Cloutier, A.W. Weimer, S.M. George, Rotary reactor for atomic layer deposition on large quantities of nanoparticles, *J. Vac. Sci. Technol. A* 25 (2007) 67-74.

[5] P. Maingon, É. Nouhaud, F. Mornex, G. Créhange, Stereotactic body radiation therapy for liver tumours, *Cancer/Radiothérapie*, 18 (2014) 313-319.

[6] T. A. Greenhalgh, R. P. Symonds, Principles of chemotherapy and radiotherapy, *Obstetrics, Gynaecology & Reproductive Medicine*, 24 (2014) 259-265.

[7] R. D. Corato, A. Espinosa, L. Lartigue, M. Tharaud, S. Chat, T. Pellegrino, C. Ménager, F. Gazeau, C. Wilhelm, Magnetic hyperthermia efficiency in the cellular environment for different nanoparticle designs, *Biomaterials*, 35 (2014) 6400-6411.

[8] E. Garaio, J.M. Collantes, J.A. Garcia, F. Plazaola, S. Mornet, F. Couillaud, O. Sandre, A wide-frequency range AC magnetometer to measure the specific absorption rate in nanoparticles for magnetic hyperthermia, *Journal of Magnetism and Magnetic Materials*, 368 (2014) 432-437.

[9] M.E. Sadat, R. Patel, S.L. Bud'ko, R.C. Ewing, J. Zhang, H. Xu, D.B. Mast, D. Shi, Dipole-interaction mediated hyperthermia heating mechanism of nanostructured  $\text{Fe}_3\text{O}_4$  composites, *Materials Letters* 129(2014) 57–60

[10] A.E. Deatsch, B.A. Evans, Heating efficiency in magnetic nanoparticle hyperthermia, *Journal of Magnetism and Magnetic Materials* 354(2014) 163–172

[11] C.S.S.R. Kumar, F. Mohammad, Magnetic nanomaterials for hyperthermia-based therapy and controlled drug delivery, *Advanced Drug Delivery Reviews* 63 (2011) 789–808.

[12] S. Laurent, S. Dutz, U.O. Häfeli, M. Mahmoudi, Magnetic fluid hyperthermia: Focus on superparamagnetic iron oxide nanoparticles, *Advances in Colloid and Interface Science* 166 (2011) 8–23.

[13] M. Veverka, P. Veverka, Z. Jiráček, O. Kaman, K. Knížek, M. Maryško, E. Pollert, K. Závěta, Synthesis and magnetic properties of  $\text{Co}_{1-x}\text{Zn}_x\text{Fe}_2\text{O}_{4+y}$  nanoparticles as materials for magnetic fluid hyperthermia, *Journal of Magnetism and Magnetic Materials*, 322 (2010) 2386-2389.

[14] C.L. Tseng, K.C. Chang, M.C. Yeh, K.C. Yang, T.P. Tang, F.H. Lin, Development of a dual-functional Pt–Fe–HAP magnetic nanoparticles application for chemo-hyperthermia treatment of cancer, *Ceramics International*, 40 (2014) 5117-5127.

[15] A.E. Deatsch, B.A. Evans, Heating efficiency in magnetic nanoparticle hyperthermia, *J. Magnetism Magnetic Mater.* 354 (2014) 163-172.

[16] H.S. Huang, J.F. Hainfeld, Intravenous magnetic nanoparticle cancer hyperthermia, *Int. J. Nanomedicine*, 8 (2013) 2521-2532.

[17] T.C. Lin, F.H. Lin, J.C. Lin, In vitro feasibility study of the use of a magnetic electrospun chitosan nanofiber composite for hyperthermia treatment of tumor cells, *Acta Biomater.* 8 (2012) 2704-2711.

[18] F. Yang, C. Jin, S. Subedi, C.L. Lee, Q. Wang, Y. Jiang, J. Li, Y. Di, D. Fu, Emerging inorganic nanomaterials for pancreatic cancer diagnosis and treatment, *Cancer Treatment Rev.* 38 (2012) 566-579.

[19] W. Rao, W. Zhang, I. Poventud-Fuentes, Y. Wang, Y. Lei, P. Agarwal, B. Weekes, C. Li, X. Lu, J. Yu, X. He, Thermally responsive nanoparticle-encapsulated curcumin and its combination with mild hyperthermia for enhanced cancer cell destruction, *Acta Biomater.* 10 (2014) 831-842.

[20] T. Sadhukha, T.S. Wiedmann, J. Panyam, Inhalable magnetic nanoparticles for targeted hyperthermia in lung cancer therapy, *Biomaterials* 34 (2013) 5163-5171.

[21] M. Bañobre-López, A. Teijeiro, J. Rivas, Magnetic nanoparticle-based hyperthermia for cancer treatment, *Reports of Practical Oncology & Radiotherapy*, 18 (2013) 397-400.

[22] C.S.S.R. Kumar, F. Mohammad, Magnetic nanomaterials for hyperthermia-based therapy and controlled drug delivery, *Adv. Drug Delivery Rev.* 63 (2011) 789-808.

[23] G. Vallejo-Fernandez, O. Whear, A. G Roca, S. Hussain, J. Timmis, V. Patel, K. O'Grady, Mechanisms of hyperthermia in magnetic nanoparticles, *J. Phys. D: Appl. Phys.* 46 (2013) 312001.